Low Temperature Physics/Fizika Nizkikh Temperatur, 2021, vol. 47, No. 5, pp. 429–434

Phase diagram of the Potts model with the number of spin states $q = 4$ on a kagome lattice

M. K. Ramazanov[1,2], A. K. Murtazaev[1,2], M. A. Magomedov[1,2], T. R. Rizvanova[1], and A. A. Murtazaeva[1]

[1]*Institute of Physics, Dagestan Federal Research Center, Russian Academy of Sciences, Makhachkala 367003, Russia*
E-mail: sheikh77@mail.ru

[2]*Dagestan Federal Research Center, Russian Academy of Sciences, Makhachkala 367000, Russia*

Received December 9, 2020, published online March 26, 2021

The magnetic structures of the ground state, phase transitions, and the thermodynamic properties of a two-dimensional ferromagnetic Potts model with the number of spin states $q = 4$ on a kagome lattice are studied using the Wang–Landau algorithm of the Monte Carlo method, taking into account the interactions of the nearest and the next-nearest neighbors. The studies were carried out for the value of the interaction of the next-nearest neighbors in the range $0 \le r \le 1.0$. It is shown that taking into account the antiferromagnetic interactions of the next-nearest neighbor leads to a violation of the magnetic ordering. A phase diagram of the dependence of the critical temperature on the value of the interaction of the next-nearest neighbor is constructed. The analysis of the character of phase transitions is carried out. It was found that in the ranges $0 \le r < 0.5$ and $0.5 < r \le 1.0$, a first-order phase transition is observed, and for $r = 0.5$, frustrations are observed in the system.

Keywords: frustration, phase diagram, phase transition, Monte Carlo method, Potts model.

1. Introduction

Recently, the study of phase transitions (PT) and low-temperature properties of compounds with a kagome lattice has attracted much attention. This is due to the fact that in such substances, due to the special geometry of the lattice, frustrations can arise. In antiferromagnetic compounds with a kagome lattice, frustrations are observed when the exchange interactions of the nearest neighbors are taken into account. In ferromagnetic compounds, frustration can appear due to antiferromagnetic interactions of the next-nearest neighbors, which compete with exchange interactions between the nearest and neighbors. Frustration effects play an important role in magnetic systems. Frustrated spin systems exhibit properties that differ from the corresponding non-frustrated systems, which arouses increased interest in the study of the phenomena of frustration in magnetic systems [1–3].

This interest is due to the fact that frustrated magnets have broad prospects for practical application [1, 4, 5]. The models of Ising, Heisenberg, Potts, and others are widely used to study the physical properties of such magnets. These models also describe a large class of real physical systems: layered magnets, liquid helium films, superconducting films, adsorbed films, etc. [1, 6, 7].

To date, the classical Ising and Heisenberg models are well studied and many of their properties are known [8–12]. The situation is different with the Potts model. In recent years, a significant number of works [6, 13–17] have been devoted to the study of spin systems described by the Potts model, in which many questions have been answered. In [13–20], the results obtained for the two-dimensional Potts model with the number of spin states $q = 2$, $q = 3$, and $q = 4$ on different types of lattices are presented. The results presented in these papers show that many of the physical properties of the Potts model depend on the value of the interaction of the next-nearest neighbors, the number of spin states q, and on the geometry of the lattice.

In this work, we investigate the two-dimensional ferromagnetic Potts model with the number of spin states $q = 4$ on the kagome lattice, taking into account the antiferromagnetic exchange interactions of the next-nearest neighbors.

The interest in this model is due to the following main reasons:

First, the question related to the type of PT for the Potts model with $q = 4$ is still controversial, since the value $q = 4$ is the boundary value of the range $2 \le q \le 4$, where a second-order PT is observed in the range $q > 4$, in which the PT occurs as a first-order phase transition [16].

Second, the nature of the PT and the thermodynamic properties for the Potts model with $q = 4$ at various values of the interaction between next-nearest neighbors have not yet been studied.

Third, taking into account the antiferromagnetic exchange interactions of the next-nearest neighbors in the model under study can lead to frustrations.

In this regard, in this work, we study this model in a wide range of values of the interaction of next-nearest neighbors. The study of this model on the base of modern methods and ideas will allow one to obtain the answer to a number of questions related to PTs and the thermodynamic properties of frustrated spin systems and systems with competing exchange interactions.

2. Model and the method of studies

The Hamiltonian of the Potts model with the number of spin states $q = 4$ which takes into account interactions of the nearest and next-nearest neighbors can be represented as [21, 22]

$$H = -J_1 \sum_{\langle i,j\rangle, i\neq j} S_i S_j - J_2 \sum_{\langle i,k\rangle, i\neq k} S_i S_k = \\ = -J_1 \sum_{\langle i,j\rangle, i\neq j} \cos\theta_{i,j} - J_2 \sum_{\langle i,k\rangle, i\neq k} \cos\theta_{i,k}, \qquad (1)$$

where J_1 and J_2 are the parameters of exchange ferro- ($J_1 > 0$) and antiferromagnetic ($J_2 < 0$) interaction of the nearest and next-nearest neighbors, $\theta_{i,j}$, $\theta_{i,k}$ are the angles between interacting spins $S_i - S_j$ and $S_i - S_k$.

The model description is shown in the inset of Fig. 1. The each spin has a four nearest (solid bold lines) and four next-nearest (dashed lines) neighbors. The four possible directions of the spins and its symbol representation also showed in the Fig. 1. The spin directions specified in such a way give the following equalities:

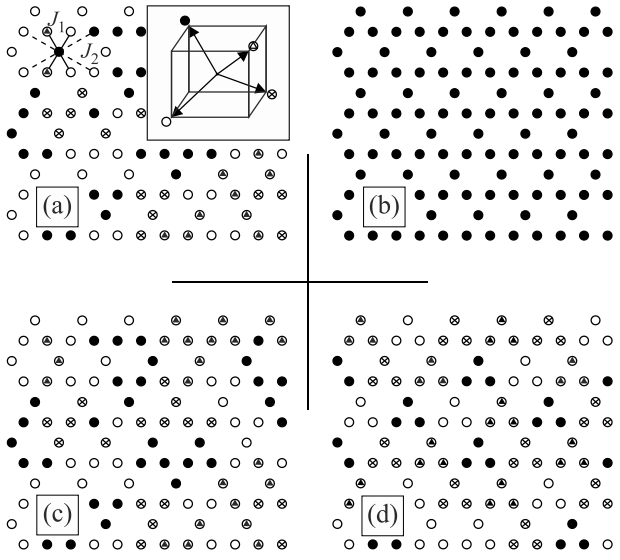

Fig. 1. Model description (a) and the magnetic structures of the ground state (b)–(d).

$$\theta_{i,j} = \begin{cases} 0, & \text{if} \quad S_i = S_j, \\ 109.47°, & \text{if} \quad S_i \neq S_j, \end{cases} \Rightarrow$$

$$\Rightarrow \cos\theta_{i,j} = \begin{cases} 1, & \text{if} \quad S_i = S_j \\ -1/3, & \text{if} \quad S_i \neq S_j \end{cases}. \qquad (2)$$

Let's introduce $r = |J_2/J_1|$ the absolute values of ratio of the nearest and of the next-nearest neighbors interactions. In this work, we consider the range of values $0 \le r \le 1.0$.

At the present time, these systems based on microscopic Hamiltonians are successfully studied basing on the Monte Carlo (MC) method [23–26]. In recent time, many new variants of algorithms of the MC methods have been developed. The Wang–Landau algorithm of the MC method is one of most efficient for studying similar systems [27], in particular, at low temperatures. Thus, we used this algorithm in this study.

The Wang–Landau algorithm is described in more detail in [15]. This algorithm allows calculate the values of thermodynamic parameters at any temperature. In particular, the internal energy U, free energy F, specific heat C, and entropy S can be calculated, using the following expressions:

$$U(T) = \frac{\sum_E Eg(E)\, e^{-E/k_BT}}{\sum_E g(E)\, e^{-E/k_BT}} \equiv \langle E\rangle_T, \qquad (3)$$

$$F(T) = -k_BT \ln\left(\sum_E g(E)\, e^{-E/k_BT}\right), \qquad (4)$$

$$C = \frac{\left(|J_1|/k_BT\right)^2}{N}\left(\langle U^2\rangle - \langle U\rangle^2\right), \qquad (5)$$

$$S(T) = \frac{U(T) - F(T)}{T}, \qquad (6)$$

where N is the number of particles, T is temperature (here and hereafter temperature is given in units $|J_1|/k_B$) (U is the normalized quantity).

The PT character was analyzed using the four-order Binder cumulant method and the histogram method of analyzing the data of the MC method [28, 29].

The calculations were performed for the systems with the periodic boundary conditions and linear sizes $L = 12$–96 and the numbers of spins $N = L\times L\times 3/4$.

3. Results of modeling

Figure 1 shows the model description [Fig. 1(a)] and the magnetic structures of the ground state for r: 0.2 [Fig. 1(b)], 0.5 [Fig. 1(c)], and 0.9 [Fig. 1(d)]. The different states of spins are indicated by different circles [see inset in Fig. 1(a)]. To indicating the various ground states we make additions to the standard Wang–Landau algorithm, which allow us to find out the magnetic structure of the ground state of the system. We calculate the density of ground states and ana-

lyze their degeneracy. Thus, we found the three areas with different degeneracy of the ground states. In the first area ($J_2 > -0.5$), the ground states are ferromagnetic and density of stated $\ln g(E) = \ln 4$ for all linear sizes, ground states are fourfold degenerated. In the second area ($J_2 < -0.5$), density of stated $\ln g(E) \propto a \ln L^2$ and ground states are degenerated. In the third area ($J_2 = -0.5$), the ground state are strongly degenerated and density of states $\ln g(E) \propto b \ln L^2$ (note, that $a << b$). We analyze each magnetic structure and save them in graphic files. For strongly degenerated states only first 100 structures. The spins marked with the same circles have the same direction. As seen in Fig. 1(b), for $r = 0.2$, ferromagnetic ordering is observed in the system. The same picture is observed in the range $0 \le r < 0.5$. At $r = 0.5$, the ferromagnetic order is violated and a disordered state is observed in the system [Fig. 1(c)]. In the range $0.5 < r \le 1.0$, «triplet ordering» is observed, which is shown in Fig. 1(d) for $r = 0.9$. "Triplet ordering" in this paper, means that the spins in triangles have the same value.

Figure 2 shows the dependence of the minimum energy $E_{\min}$ on the value of the interaction of the next-nearest neighbors J_2. Three different structures of magnetic spin ordering are observed for the model under study, depending on the value of J_2. The figure shows that for $J_2 < -0.5$ a triplet magnetic structure is observed, and for $J_2 > -0.5$ it is ferromagnetic. At a value of $J_2 = -0.5$, the magnetic ordering is violated, which indicates that this value of J_2 are the frustration point.

The temperature dependences of entropy S are shown in Fig. 3 (hereinafter the statistic error does not exceed the sizes of the symbols of the presented dependences). As can be seen in the figure, for the entire considered range of r values, the entropy tends to the theoretically predicted value of ln 4 with increasing temperature. In the range $0 \le r < 0.5$ in the low-temperature region, the entropy tends to zero. This means that in the given range of r there is no degeneracy of the ground state and the system is not frustrated. In the range $0.5 < r \le 1.0$, the entropy tends to a nonzero value.

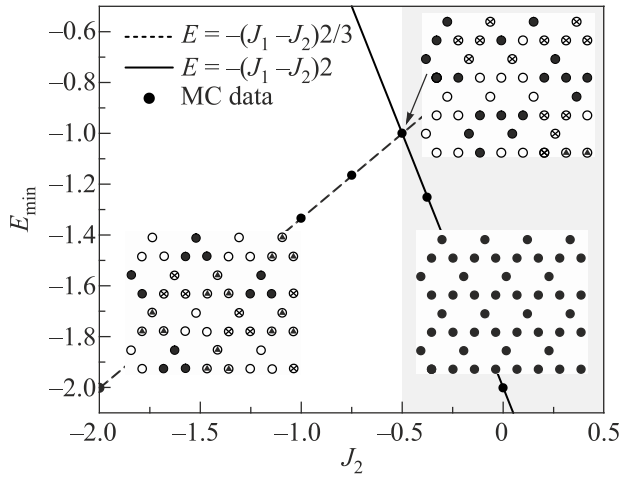

Fig. 2. Dependence of the minimum energy $E_{\min}$ on the value of the interaction of the next-nearest neighbors J_2.

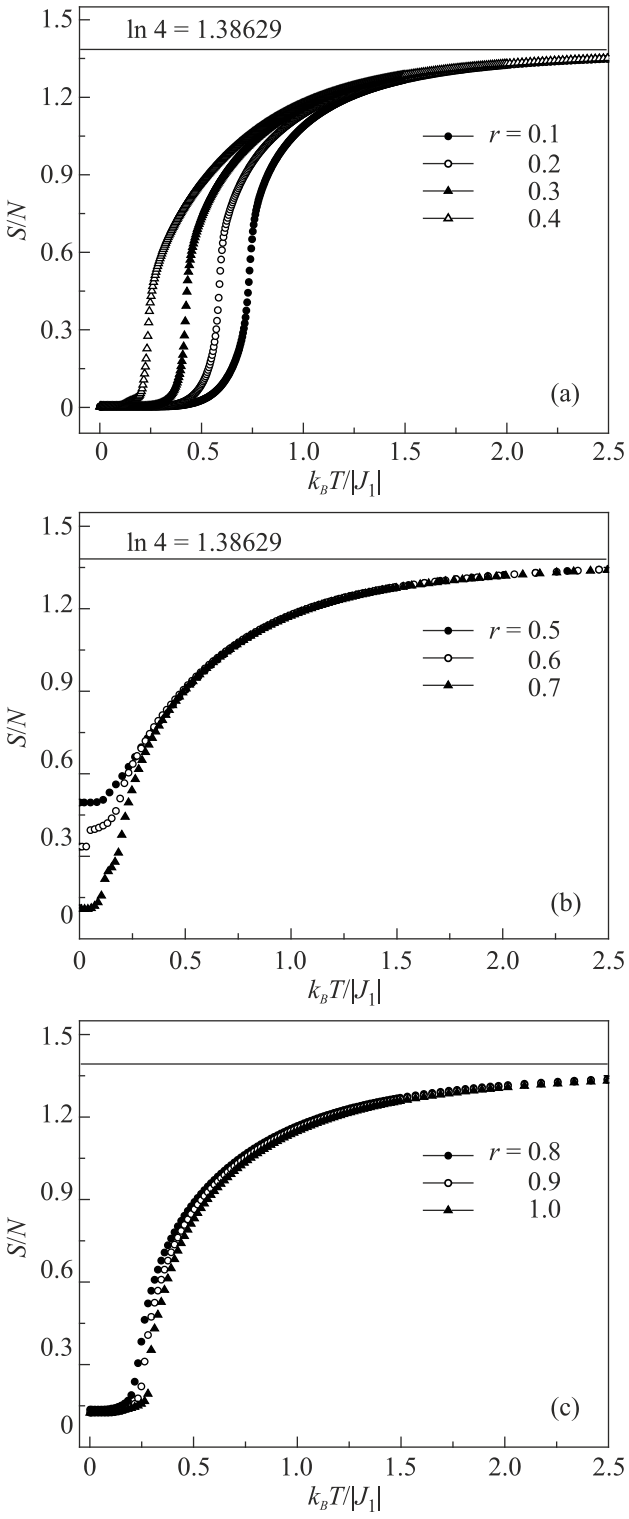

Fig. 3. Temperature dependences of the entropy S/N.

This behavior of entropy indicates that the ground state of the system is degenerated in this range and frustrations may arise in the system.

Figure 4 shows the temperature dependences of the heat capacity C for different values of r. As can be seen from the figure, for all values of r in the ranges $0 \le r < 0.5$ and $0.5 < r \le 1.0$, distinct maxima are observed near the critical point. In the range $0 \le r < 0.5$, an increase in r is accompa-

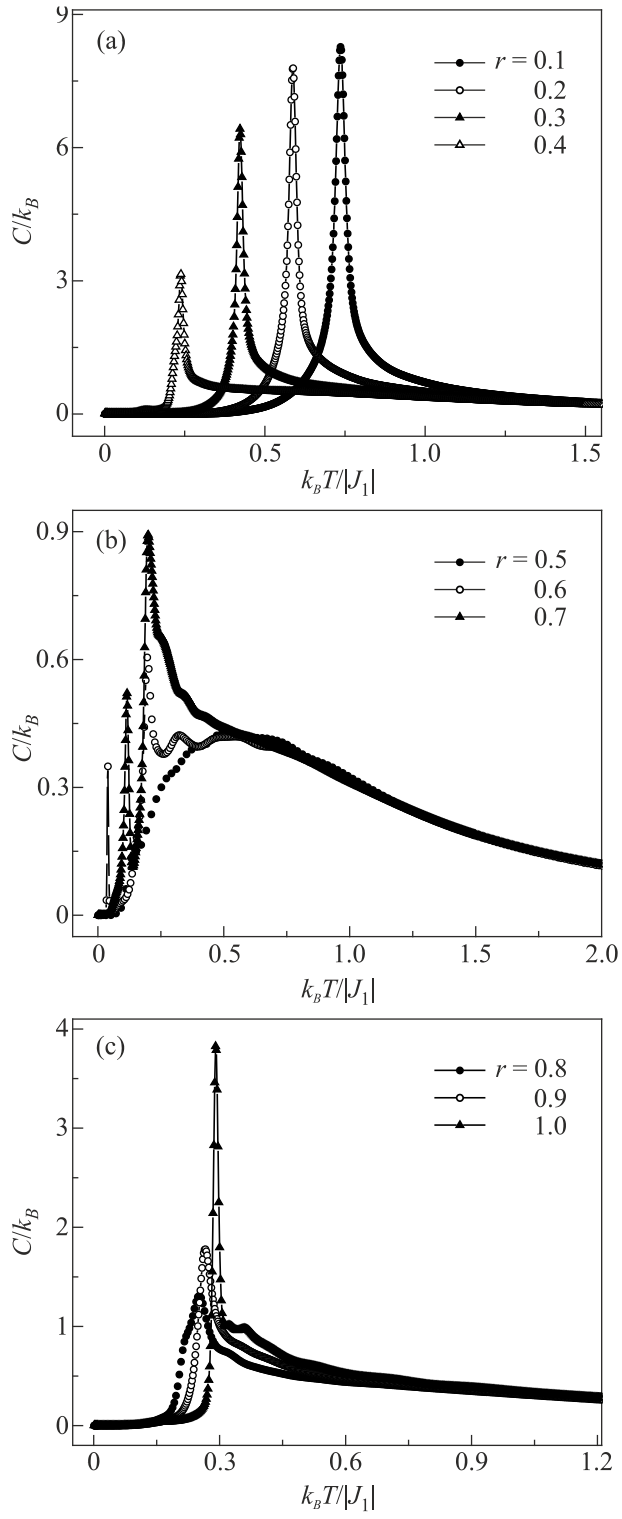

Fig. 4. Temperature dependences of the specific heat C/k_B.

nied by a shift of the maxima towards lower temperatures and a decrease in the amplitude of the maxima. The opposite picture is observed in the range $0.5 < r \leq 1.0$, where the maxima shift towards higher temperatures. For $r = 0.5$, an unusual behavior is observed, which is characterized by the absence of a pronounced peak. In this case, the heat capacity maxima have smoothed peaks instead of sharp

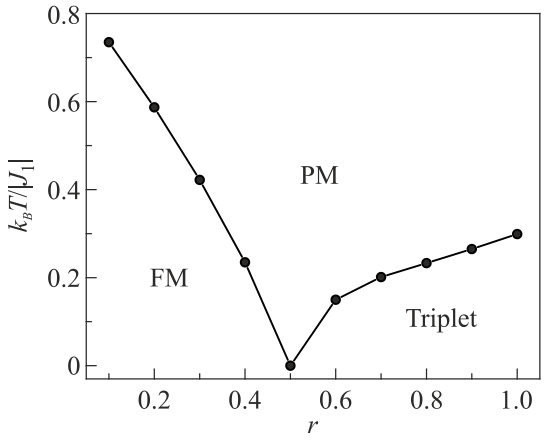

Fig. 5. Phase diagram of the dependence of the critical temperature on the value of the interaction of the next-nearest neighbors.

λ-shaped peaks. Such a picture of the temperature dependence of the specific heat is usually observed for frustrated spin systems [30]. Based on this, we can assume that the value $r = 0.5$ is the point of frustration for this model. For $r = 0.6$, a splitting of the heat capacity is observed, which is a characteristic feature of frustrated systems near the points of frustration. One maximum is sharp, and the second is smooth. This behavior is explained by the partial ordering of the system [Fig. 1(c)]. For $r = 0.5$, the effects of frustration are most pronounced, there is no sharp peak, a smoothed maximum is observed, the system passes into a highly frustrated state, i.e., there is no order in the system.

The phase diagram of the dependence of the critical temperature on the value of the interaction of the next-nearest neighbors is shown in Fig. 5. The diagram shows three different phases: ferromagnetic, paramagnetic, and triplet. For $r = 0.5$, the critical temperature is zero and there is no PT. This is explained by the fact that the competition of exchange interactions of the nearest and next-nearest neighbors in this model leads to complete frustration. Frustrations disturb the order in the system and lead to the disappearance of the PT.

To analyze the type of PT, we used the histogram analysis of the MC data [27, 28]. This method allows you to reliably determine the type of PT. The method for determining the type of PT by this method is described in detail in [31, 32].

The results obtained on the basis of the histogram analysis of the data show that a first-order PT is observed in this model. This is shown in Fig. 6. This figure shows the histograms of energy distribution for a system with linear dimensions $L = 96$ for $r = 0.2$. The plot is plotted near the critical temperature. It can be seen from Fig. 6, the dependence of the probability W of the energy E has the two maxima, and this fact favors the first-order PT. The existence of a double peak in the histograms of energy distribution is a sufficient condition for a first-order PT. Note that, double peaks in the distribution histograms for the model under

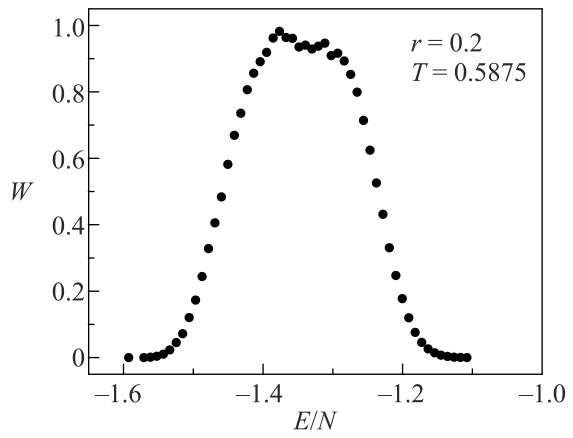

Fig. 6. Energy distribution histogram for $L = 96$.

study are observed for r values in the ranges $0 \le r < 0.5$ and $0.5 < r \le 1.0$. This allows us to state that the first-order PT observed in the was considered ranges of r values.

4. Conclusions

The magnetic structures of the ground state, the phase transitions, and the thermodynamic properties of the two-dimensional Potts model with the number of spin states $q = 4$ on a kagome lattice taking into account the interactions of the nearest and the next-nearest neighbors, have been performed using the Wang–Landau algorithm of the Monte Carlo method. The magnetic structures of the ground state are obtained in a wide range of values of the interaction the next-nearest neighbors. A phase diagram of the dependence of the critical temperature on the value of the interaction of the next-nearest neighbors is constructed. It is shown that a first-order phase transition is observed in the ranges $0 \le r < 0.5$ and $0.5 < r \le 1.0$. For $r = 0.5$, the ground state is strongly degenerates, and the system becomes frustrated.

Acknowledgments

This research was performed with financial support from the Russian Foundation for Basic Research, as part of scientific projects No. 19–02–00153-a.

1. H. T. Diep, *Frustrated Spin Systems*, World Scientific Publishing Co. Pte. Ltd., Singapore (2004), p. 624.
2. F. A. Kassan-Ogly, A. K. Murtazaev, A. K. Zhuravlev, M. K. Ramazanov, and A. I. Proshkin, *J. Magn. Magn. Mater.* **384**, 247 (2015).
3. A. K. Murtazaev, M. K. Ramazanov, and M. K. Badiev, *Phys. B, Condens. Matter* **476**, 1 (2015).
4. R. J. Baxter, *Exactly Solved Models in Statistical Mechanics*, Academic, New York (1982); Mir, Moscow (1985).
5. F. Y. Wu, *Exactly Solved Models, A Journey in Statistical Mechanics*, World Scientific, New Jersey (2008).
6. F. Y. Wu, *Rev. Mod. Phys.* **54**, 235 (1982).
7. W. Zhang and Y. Deng, *Phys. Rev. E* **78**, 031103 (2008).
8. A. K. Murtazaev, M. K. Ramazanov, D. R. Kurbanova, M. A. Magomedov, and K. Sh. Murtazaev, *Mater. Lett.* **236**, 669 (2019).
9. M. K. Ramazanov and A. K. Murtazaev, *JETP Lett.* **109**, 589 (2019).
10. A. K. Murtazaev, M. K. Ramazanov, and M. K. Badiev, *Fiz. Nizk. Temp.* **45**, 1493 (2019) [*Low Temp. Phys.* **45**, 1263 (2019)].
11. M. K. Badiev, A. K. Murtazaev, M. K. Ramazanov, and M. A. Magomedov, *Fiz. Nizk. Temp.* **46**, 824 (2020) [*Low Temp. Phys.* **46**, 693 (2020)].
12. A. K. Murtazaev, D. R. Kurbanova, and M. K. Ramazanov, *J. Exp. Theor. Phys.* **129**, 903 (2019).
13. M. Nauenberg and D. J. Scalapino, *Phys. Rev. Lett.* **44**, 837 (1980).
14. J. L. Cardy, M. Nauenberg, and D. J. Scalapino, *Phys. Rev. B* **22**, 2560 (1980).
15. M. K. Ramazanov, A. K. Murtazaev, and M. A. Magomedov, *Phys. A* **521**, 543 (2019).
16. H. Feldmann, A. J. Guttmann, I. Jensen, R. Shrock, and S.-H. Tsai, *J. Phys. A* **31**, 2287 (1998).
17. F. A. Kassan-Ogly and A. I. Proshkin, *Phys. Solid State* **60**, 1090 (2018).
18. A. K. Murtazaev, M. K. Ramazanov, M.K. Mazagaeva, and M. A. Magomedov, *J. Exp. Theor. Phys.* **129**, 421 (2019).
19. A. K. Murtazaev, D. R. Kurbanova, and M. K. Ramazanov, *Phys. Solid State* **61**, 2172 (2019).
20. M. K. Ramazanov, A. K. Murtazaev, M. A. Magomedov, and M.K. Mazagaeva, *Phys. Solid State* **62**, 499 (2020).
21. M. G. Townsend, G. Longworth, and E. Roudaut, *Phys. Rev. B* **33**, 4919 (1986).
22. Y. Chiaki and O. Yutaka, *J. Phys. A, Math. Gen.* **34**, 8781 (2001).
23. R. Masrour and A. Jabar, *Physica A* **515**, 270 (2019).
24. M. K. Ramazanov and A. K. Murtazaev, *JETP Lett.* **106**, 86 (2017).
25. A. K. Murtazaev, D. R. Kurbanova, and M. K. Ramazanov, *Physica A* **545**, 123548-1 (2020).
26. R. Masrour and A. Jabar, *Physica A* **491**, 926 (2018).
27. F. Wang and D. P. Landau, *Phys. Rev. E* **64**, 056101 (2001).
28. F. Wang and D. P. Landau, *Phys. Rev. Lett.* **86**, 2050 (2001).
29. K. Binder and D. Heermann, *Monte Carlo Simulation in Statistical Physics, An Introduction*, Springer, Berlin, Heidelberg (2010).
30. F. A. Kassan-Ogly, B. N. Filippov, A. K. Murtazaev, M. K. Ramazanov, and M. K. Badiev, *J. Magn. Magn. Mater.* **324**, 3418 (2012).
31. M. K. Ramazanov and A. K. Murtazaev, *JETP Lett.* **103**, 460 (2016).
32. A. K. Murtazaev, T. R. Rizvanova, M. K. Ramazanov, and M. A. Magomedov, *Phys. Solid State* **62**, 1434 (2020).

Фазова діаграма моделі Поттса з числом спінових станів $q = 4$ на ґратці кагоме

M. K. Ramazanov, A. K. Murtazaev,
M. A. Magomedov, T. R. Rizvanova,
A. A. Murtazaeva

Магнітні структури основного стану, фазові переходи та термодинамічні властивості двовимірної феромагнітної моделі Поттса з числом спінових станів $q = 4$ на ґратці кагоме вивчаються за допомогою алгоритму Ванга–Ландау методу Монте-Карло. Цей метод враховує взаємодію найближчих та наступних найближчих сусідів. Дослідження проводили для значення взаємодії у діапазоні $0 \le r \le 1{,}0$. Показано, що врахування антиферомагнітних взаємодій наступного найближчого сусіда призводить до порушення магнітного упорядкування. Побудовано фазову діаграму залежності критичної температури від величини взаємодії наступного найближчого сусіда. Проведено аналіз характеру фазових переходів. Було встановлено, що в діапазонах $0 \le r < 0{,}5$ та $0{,}5 < r \le 1{,}0$ спостерігається фазовий перехід першого роду, а при $r = 0{,}5$ у системі спостерігаються фрустрації.

Ключові слова: фрустрація, фазова діаграма, фазовий перехід, метод Монте-Карло, модель Поттса.